Phase Diagram of Random Copolymer Melts: A Computer Simulation Study

J. Houdayer

Service de Physique Théorique, Bat 774, Ormes des Merisiers, F-91191 Gif sur Yvette, Cedex, France

M. Müller*

Institut für Physik, WA 331, Johannes Gutenberg Universität, D-55099 Mainz, Germany

Received December 2, 2003; Revised Manuscript Received March 10, 2004

ABSTRACT: We investigate the phase behavior of random copolymer melts via large-scale Monte Carlo simulations. The AB multiblock copolymers have, on average, symmetric composition and are characterized by a correlation λ along the polymer. We employ parallel tempering and the wormhole algorithm and a technique to reduce the variance between different realizations of the disorder to explore the phase behavior. For a very large correlation of blocks, we observe a sequence of disordered phase, macrophase separation and remixing into a spatially structured (lamellar or microemulsion-like) phase upon increasing the incompatibility between different monomer species as predicted by mean field theory. For smaller values of λ, we find that a locally segregated structure gradually forms as the incompatibility increases. As we increase the number of blocks in the polymers, the region of macrophase separation shrinks. The results of our Monte Carlo simulation are in agreement with a Ginzburg criterion, which suggests that mean field theory becomes *worse* as the number of blocks in a polymer increases. Different scenarios for the remixing at large incompatibility χ have been investigated. The simulation data exhibit large finite size effects. Depending on the parameters, the remixing might be either an unbinding transition, where the characteristic length scale of the spatially structured phase diverges, or a three-phase coexistence over an extended range of incompatibilities. In the latter case, the sequence distribution in the coexisting phases differs (fractionation).

I. Introduction

In polymeric systems one often encounters phase equilibria in mixtures with a large number of components. For instance, polydispersity, i.e., a continuous distribution of chain lengths, alters the phase equilibrium between a dense polymer phase and its vapor.[1] Random AB copolymers constitute another example of such mixtures; each sequence of A's and B's represents a different component. The phase behavior of random copolymers has attracted abiding interest because these systems are produced commercially in large amounts.[2] They are expected to exhibit a rich phase behavior. Mean field calculations predict a disordered phase, macrophase separation, and a spatially structured phase as a function of the incompatibility χ of the different constituents A and B and the correlation λ along the polymer.[3−6]

In a recent Monte Carlo simulation we explored the phase behavior of random copolymers.[7] In fact, we observed all three phases predicted by mean field calculations for short chain lengths. Upon increasing the number of blocks in a molecule, however, the stability region of the macrophase-separated state decreased, in marked contrast to the mean field predictions. Using a Ginzburg criterion,[8] we showed that the mean field behavior is not self-consistent in the limit of many blocks and that the disordered, spatially structured state is stable in a large region of parameter space. Random copolymers are one of the very few examples of a dense macromolecular mixture in which mean field theory *qualitatively* fails.

Computer simulations appear ideally suited to explore the phase behavior in the framework of a well-defined model system, but the simulation of random copolymer melts is a difficult task. (i) Dense polymer systems suffer from a slow relaxation of chain conformations. Moreover, the extended molecules require a rather large spatial extension of the simulation cell. (ii) One encounters typical problems associated with disordered systems—large finite size effects and the need for averaging over realizations of disorder. Moreover, theoretical approaches[9−11] and simulations[12] of random copolymers observe a slow glassy frozen-in dynamics at low temperatures. (iii) Due to the large number of chemically different species, the phase behavior might be quite intricate—phase coexistence between many different phases each of which is characterized by a distribution of sequences has to be considered.

To address all these difficulties, we used sophisticated techniques (such as parallel tempering[13]) and developed new ones such as the wormhole algorithm[14] and the disorder variance reduction (described below). Altogether the results presented here required around 25 years of single processor CPU time on a Cray-T3E. These results would have been completely out of reach with standard techniques.

Our manuscript is arranged as follows: First, we give a detailed account of the computational techniques. Then we extend our simulations to corroborate the Ginzburg criterion for the macrophase transition. Subsequently, we explore the transition from the macrophase-separated state to the spatially structured phase at lower temperatures. We close with a brief outlook on open questions.

* To whom correspondence should be addressed.

10.1021/ma035814p CCC: $27.50
Published on Web 05/01/2004

II. Model

A. Dense Random Copolymer Melt. We consider a dense melt of linear polymers, all composed of N monomers of two different kinds, A and B. A- and B-monomers are structurally symmetric, i.e., they have identical shape and bonds, but different types repel each other. The strength of the monomeric repulsion is characterized by the Flory−Huggins parameter χ.

We will use the same model as employed by Fredrickson, Milner, and Leibler.[5] Polymers consist of Q blocks. Each block is made of either M A-monomers or M B-monomers, and thus, the total chain length is $N = QM$. The actual sequence of blocks is fixed independently for each polymer by a random polymerization process. Note that these sequences no longer evolve once the polymerization process is completed. The sequence along a polymer is quenched. The overall composition of the mixture is described by a parameter f ($0 \le f \le 1$), and the probability for a given segment to be an A-segment (or a B-segment) is $f_A = f$ (or $f_B = 1 - f$). The random Markovian polymerization process is defined by the conditional probability $P_{\alpha\beta}$ of adding a β-segment after an α-segment (independent of the rest of the chain). This is parametrized by the correlation coefficient λ between two neighboring blocks ($-1 \le \lambda \le 1$). $\lambda = 1$ gives rise to fully correlated blocks (and hence homopolymers); $\lambda = -1$ yields alternating sequences ABABABAB... (here $M = 1$), and for $\lambda = 0$ the blocks are uncorrelated. More precisely we have

$$P_{AB} = rf_B \tag{1}$$

$$P_{BA} = rf_A \tag{2}$$

$$P_{AA} = 1 - rf_B \tag{3}$$

$$P_{BB} = 1 - rf_A \tag{4}$$

with $r = 1 - \lambda$. In the following we do not consider degenerate cases such as $|\lambda| = 1$ or $f = 0$ or 1.

In the symmetric case $f = 1/2$, these equations simplify to

$$P_{AA} = P_{BB} = p \tag{5}$$

$$P_{AB} = P_{BA} = q \tag{6}$$

with $p = (1 + \lambda)/2$ and $q = (1 - \lambda)/2$. Then, the sequence distribution is characterized by a single value, λ, and we will denote this distribution of sequences a λ-distribution in the following.

For given values of the parameters N, Q, M, f, and λ, the system may contain up to n different kinds of polymers (each kind corresponding to a possible sequence of A's and B's) with

$$n = 2^{Q-1} + 2^{[Q/2]-1} \tag{7}$$

where $[x]$ denotes the smallest integer greater than or equal to x. The number of sequences n grows exponentially with Q; for example, $n = 3$, 6, 20, 528, and 524 800 for $Q = 2$, 3, 5, 10, and 20, respectively. Since each sequence corresponds to a different chemical species, the model is an n-component mixture. Actually, in the thermodynamical limit (i.e., large volume limit), each possible sequence S will be present a large number of times $N_S = \rho_S N_p$, where N_p is the total number of polymers and ρ_S is the relative concentration of species S. In this limit, $\rho_S = P(S)$ with $P(S)$ being the probability for the random copolymerization process to produce sequence S

$$P(S) = r^k f_A^{S_A} f_B^{S_B} (1 - rf_B)^{N_A - S_A} (1 - rf_A)^{N_B - S_B} \tag{8}$$

with k the number of A−B bonds in S, S_A (S_B) the number of continuous A (B) sequences in S, and N_A (N_B) the number of A (B) blocks in S. For example, if $M = 1$ and S = AAABBAABAA, then k, S_A, S_B, N_A, and N_B take the values 4, 3, 2, 7, and 3, respectively.

It is crucial to comment that in the thermodynamical limit,[15] the ρ_S's are *not* random variables. They are uniquely defined by the $P(S)$'s, and since the nature of the system is entirely defined by the ρ_S's, it is *not* a disordered system: There is *no* quenched disorder. The situation would be quite different if, for example, the centers of mass of the polymers would be pinned on a lattice or if we would consider a single random copolymer in the large Q limit. In those cases there would be quenched disorder. The two important points in our system are (i) the polymers can freely move, and hence no local property is frozen; (ii) the large volume limit is taken before the large Q limit, so that each possible species is present a large number of times in the mixture.

On the other hand, the local concentrations of the different species may, of course, fluctuate in space independently of one another. In the case of a phase separation, the composition of one of the phases cannot be described by a small set of parameters such as f and λ. One has, in general, to determine the whole set of ρ_S for each phase.

B. Bond Fluctuation Model. To represent this model we use for simplicity and computational efficiency a lattice description, namely, the bond fluctuation model.[16] The phase behavior[17] and interface properties[18] of homopolymer mixtures and diblock copolymers[19] have been studied in the framework of this coarse-grained model, and the simulation results have been compared to mean field predictions of the Gaussian chain model without any adjustable parameter.

Space is described as a 3-dimensional cubic lattice of size $L \times L \times L$ with periodic boundary conditions. Each monomer is represented by a $2 \times 2 \times 2$ cube on this lattice, and the short-ranged repulsion (excluded volume) is represented by an infinite overlap potential (i.e., the cubes cannot overlap). To represent a melt we set the density to $\rho = 1/16$ (i.e., the total number of monomers is ρL^3, $N_p = \rho L^3/N$, and one-half of the sites are occupied). Monomers are connected by one of 108 bond vectors with lengths 2, $\sqrt{5}$,$\sqrt{6}$, 3, and $\sqrt{10}$ (namely, (2, 0, 0), (2, 1, 0), (2, 1, 1), (2, 2, 1), (3, 0, 0), and (3, 1, 0) and all symmetry-related ones). The interactions between the monomers are represented by a short-ranged square-well potential which encompasses the 54 nearest-neighboring sites of a given monomer. The strength $\epsilon_{\alpha\beta}$ of the potential depends on the nature of the monomers involved. We set $\epsilon_{AB} = \epsilon_0$ and $\epsilon_{AA} = \epsilon_{BB} = 0$. We choose to have no attraction between the monomers to avoid complications in which we are not interested, such as condensation into a dense polymer liquid and a vapor or crystallization. Note that phase separation occurs at $\epsilon \approx 1/M$. If we included attractive interactions, the liquid−liquid demixing might interfere (for small M) with the liquid−vapor phase separation below the Θ-temperature.

The interactions are related to the Flory−Huggins parameter χ through $\chi = z\epsilon_0/k_BT$, where z is the number of intermolecular contacts per monomer

$$z = \rho \int_{r \le \sqrt{6}} d^3\mathbf{r}\, g^{\text{inter}}(r) \tag{9}$$

where g^{inter} denotes the intermolecular pair-correlation function.[20] Due to the correlation hole effect it depends slightly on the chain length N but is to a good approximation independent from the other model parameters. We measured $z = 3.20$, 3.04, 2.91, 2.83, and 2.67 for $N = 5$, 8, 10, 12, and 20, respectively.

III. Simulation Technique

To study this system, we performed extensive parallel Monte Carlo simulations on a Cray-T3E. This problem is quite demanding, and we had to develop specific new Monte Carlo techniques to tackle it. We present here the details of these simulations.

A. Statistical Ensembles. The choice of the simulation ensemble is a delicate issue. On one hand, the canonical ensemble (where the global concentration of each component is kept fixed) is generally not adapted to investigate macrophase separation. The difficulty arises from the fact that coexisting phases would simultaneously be present in the simulation cell together with interfaces between them. Any precise measurement of the location and information about the nature of the phase transitions would require inaccessibly large simulation cells. This problem would be particularly acute in our case since we expect only a weak segregation between the macrophases and extremely wide interfaces. Additionally, concentration fluctuations relax only via the slow diffusive motion of molecules.

On the other hand, the grandcanonical ensemble (where the global concentrations of the components can vary independently) is hampered by the large number, n, of different chemical species in the system (see eq 7). In the grandcanonical ensemble one needs to choose n independent chemical potentials, μ_S, in such a way that the concentrations of the n components correspond to the values of interest of λ and f. In principle, we could determine the values of the μ_S from a canonical simulation, but obtaining the required precision is difficult particularly when the temperature is low (i.e., large χ) and the concentrations of the individual components are small. Those methods have been used for polydisperse fluids[21] of size-dispersed hard spheres and in an approximate way also for chain molecules.[22]

In the present work we choose the two following ensembles.

(1) Extended Canonical Ensemble. To simplify the problem, we restrict ourselves to strictly symmetric mixtures, i.e., $f = 1/2$. This introduces the following symmetry in the system: Consider a component of sequence S, we define $\bar{S}$ to be the symmetric sequence replacing all A's by B's and all B's by A's. For example, if S = AABBA then $\bar{S}$ = BBAAB. Then we have

$$\mu_{\bar{S}} = \mu_S \tag{10}$$

This means that any phase of the system must be either symmetric or coexists with its symmetric.

We define the extended canonical ensemble (ECE) as follows: It is a canonical ensemble with additional degrees of freedom. More precisely, we allow polymers of sequence S to be replaced by polymers of sequence $\bar{S}$ and vice versa, with the constraint that the total numbers of polymers S and $\bar{S}$ are constant for each sequence. Another way to understand this is to consider another system where the sequences S and $\bar{S}$ are the same chemical species with an internal Ising degree of freedom $\sigma = \pm 1$ (say $\sigma = +1$ for S and $\sigma = -1$ for $\bar{S}$). Then our ECE is the canonical ensemble for this new system, whereas the canonical ensemble for the original system corresponds to the freezing of these spins (i.e., fixed "magnetization"). In this new system the number $\bar{n}$ of components is

$$\bar{n} = 2^{Q-2} + 2^{[Q/2]-1} \tag{11}$$

with $[x]$ being the largest integer less than or equal to x. This gives, for example, $\bar{n} = 2$, 3, 10, 264, and 262 400 for $Q = 2$, 3, 5, 10, and 20, respectively.

With this ensemble we can investigate the macrophase separation of our system, since when there are two coexisting phases they must be symmetric. They will no longer coexist simultaneously in our simulation cell, and the system will go from one to the other in the course of the simulation. In the case where more than two phases coexist, we again observe simultaneously several phases in the simulation cell. In fact, there may be up to n coexisting phases in the system and up to $\bar{n}$ in the simulation cell.

2. Semi-Grandcanonical Ensemble. To investigate parameter values where more than two phases coexist, we need a grandcanonical ensemble. For simplicity and since we are interested in the dense regime (melt), we choose the semi-grandcanonical ensemble (SGCE) (where the total number of polymers is fixed). To decrease the number of parameters, we again set $f = 1/2$, and thus, we have $\bar{n} - 1$ independent chemical potentials (see eq 11). In practice, we are then restricted to very small values of Q, i.e., $Q < 4$.

B. Monte Carlo Moves. We employ five different kinds of moves.

(i) We use standard local moves: Take a monomer at random; try to move it to a neighboring lattice site accept with the Metropolis criterion, namely, with probability

$$P = \min[1, \exp(-\Delta K)] \tag{12}$$

with $\Delta K = \beta \Delta E$, where $\beta = 1/k_BT$ and ΔE is the energy difference produced by the move.

(ii) To relax the configurations of the polymers efficiently, we use the recently devised "wormhole" algorithm.[14] It extends and generalizes the "slithering snake" algorithm to complex polymer architectures and allows for a fast and efficient relaxation of the configurations even in the case of multiblock copolymers.

(iii) To circumvent the slow dynamics at low temperature (i.e., large χ), we use exchange Monte Carlo[13] (also called parallel tempering): Simulate different temperatures in parallel. The move consists of taking two neighboring temperatures and exchanging the configurations according to eq 12 with

$$\Delta K = -(\beta_2 - \beta_1)(E_2 - E_1) \tag{13}$$

for ECE and

$$\Delta K = -(\beta_2 - \beta_1)(E_2 - E_1) + \sum_S (N_{S,2} - N_{S,1})(\beta_2 \mu_{S,2} - \beta_1 \mu_{S,1}) \quad (14)$$

for SGCE. Indices 1 and 2 denote the two configurations.

(iv) In the ECE, we choose a polymer at random and try to replace it by its symmetric $S \rightarrow \bar{S}$ and accept with $\Delta K = \beta \Delta E$. In the SGCE, we take a polymer at random and try to replace it by a randomly chosen sequence $S \rightarrow S'$ and accept the move with $\Delta K = \beta(\Delta E - \Delta\mu)$, where $\Delta\mu = \mu_{S'} - \mu_S$.

(v) In the ECE, we also use an exchange move to mix the sequences of the polymers. It works as follows: Take two polymers at random in the cell and try to exchange them. If the two sequences are S_1 and S_2, this means $S_1 \rightarrow S_2$ and $S_2 \rightarrow S_1$. The move is accepted with $\Delta K = \beta \Delta E$. It is possible to optimize this move by a priori choosing between different possibilities (and still enforcing detailed balance). If we note $-S$ the reverse of sequence S (i.e., if S = AAABA, $-S$ = ABAAA), we can also try ($S_1 \rightarrow -\bar{S}_2$ and $S_2 \rightarrow -\bar{S}_1$). We can even mix this move with move iv and try the symmetric sequences: ($S_1 \rightarrow \bar{S}_2$ and $S_2 \rightarrow \bar{S}_1$) or even ($S_1 \rightarrow -\bar{S}_2$ and $S_2 \rightarrow -\bar{S}_1$). Between all these possibilities, only the one that minimizes the number of monomers that actually change is attempted. For example, if S_1 = AAABA and S_2 = AABBB, the different possibilities, respectively, change 4, 8, 6, and 2 monomers, so only the last one is actually tried, thus increasing the acceptance rate of the move (note that the increase of computer time needed to do one move is negligible compared to the computation time of the energy difference). Finally, other possibilities such as ($S_1 \rightarrow -S_2$ and $S_2 \rightarrow S_1$) or ($S_1 \rightarrow \bar{S}_2$ and $S_2 \rightarrow S_1$) are not considered because they would always change more monomers than the others.

C. Disorder Variance Reduction. At the beginning of the simulation one must choose the number N_S of polymers with sequence S present in the simulation cell. In both ensembles, we set the total number of polymers to $N_p = \sum_S N_S = \rho L^3/N$. In SGCE, the choice of the initial N_S's is irrelevant since they relax during the simulation. On the other hand, in ECE one must choose each N_S or more precisely each $N_S + N_{\bar{S}}$. Of course, they must be chosen according to Q, M, λ, and f, but how?

A straightforward approach would be to produce each sequence independently simply using the definitions of Q, M, λ, and f: Choose the first segment randomly according to f, then choose the second randomly according to $P_{\alpha\beta}$, and so on until you have Q blocks. In the thermodynamic limit (i.e., infinite volume), we would always get the same relative concentration $\rho_S = N_S/N_p$ of each sequence, namely, $\rho_S = P(S)$, where $P(S)$ is the probability of creating sequence S according to the random polymerization process. Note again that in this limit the system is *not* a disordered system since all information is contained in Q, M, λ, and f (and χ). The problem is that we are *not* in the thermodynamic limit and generally $\rho_S \neq P(S)$. For instance, for $Q = 5$, $M = 4$, and $L = 40$, there are 20 distinct sequences but the simulation cell contains only 200 polymers. Therefore, there are fluctuations and any measured physical quantity depends on the actual values of the ρ_S's. This effect is unfortunately not small at all and cannot be neglected (see below). An average over different realizations of the disorder would be required, but this entails a tremendous increase of computation time.

Another way would be to try to directly set the ρ_S's to their limiting values (namely, $\rho_S = P(S)$); this would remove all fluctuations without changing the thermodynamic limit and no average would be necessary. Unfortunately, this approach is not possible because the number of species n is very large (see eq 7), and thus, $N_p P(S)$ is smaller than 1 for most of the sequences, whereas the values of N_S are of course integers.

We propose here an intermediate procedure to reduce the fluctuations. It consists of grouping the different sequences into classes of similar sequences. (In the following, we consider a sequence S and its reverse $-S$ to be distinct.) For these classes we require the following properties: Sequences in one class C must have similar physical properties, the $P(S)$'s must all be equal inside one class (we note $P_C = P(S)$ for any $S \in C$), and the number of classes must be small. If these conditions are met, we can do the following: For a class C, the limiting concentration of class C is $\rho_C = n_C P_C$ (with n_C the number of sequences in C) and the number of sequences chosen in class C should be $N_C \simeq \rho_C N_p$, which should be reasonably large if the number of classes is small. Once the N_C's are chosen (rounding to integer values in some reasonable way such that $\sum N_C = N_p$), we repeatedly produce a sequence using the random polymerization process and add it to the mixture if the corresponding class is not complete, and we stop when all classes are fully populated. The important point is that this procedure is *not* an approximation in itself in the sense that in the thermodynamic limit it yields exactly the correct ρ_S values, and thus, we obtain correct limiting values for any physical observable. What we hope here is that fluctuations for finite size systems are small enough so that averaging over different realizations of the disorder is no longer necessary.

Let us now come to the classes we choose. In the following, we consider only the case $M = 1$; generalization to larger M is straightforward. We characterize a sequence S by three parameters: $m = N_B - N_A$ the excess number of B's in S, k defined, as before, as the number of A−B bonds in S (for example if S = AABAB then $k = 3$: AA−B−A−B), and when k is even, α the type (A or B) of the end monomers (which are both identical—A or B—in this case). For example, AAABBABA has $m = -2$, $k = 4$, and α = A. A class $C(m, k)$ (or $C(m, k, \alpha)$ for even k) is the set of all sequences having these values of the parameters. From eq 8, we have

$$P_C = r^k f_A^{S_A} f_B^{S_B} (1 - r f_B)^{N_A - S_A} (1 - r f_A)^{N_B - S_B} \quad (15)$$

where $N_A = (Q - m)/2$ and $N_B = (Q + m)/2$ are the number of A's and B's. S_A and S_B are the number of continuous sequences of A's and B's. If k is odd, $S_A = S_B = (k + 1)/2$, otherwise $S_\alpha = k/2 + 1$ and $S_{\bar{\alpha}} = k/2$. Moreover, when $f = 1/2$, this simplifies to

$$P_C = \frac{1}{2} q^k p^{Q-k-1} \quad (16)$$

which is independent of m and α. Finally, we have

$$n_C = \gamma \binom{N_A - 1}{S_A - 1} \binom{N_B - 1}{S_B - 1} \quad (17)$$

with $\gamma = 2$ for odd k and $\gamma = 1$ otherwise.

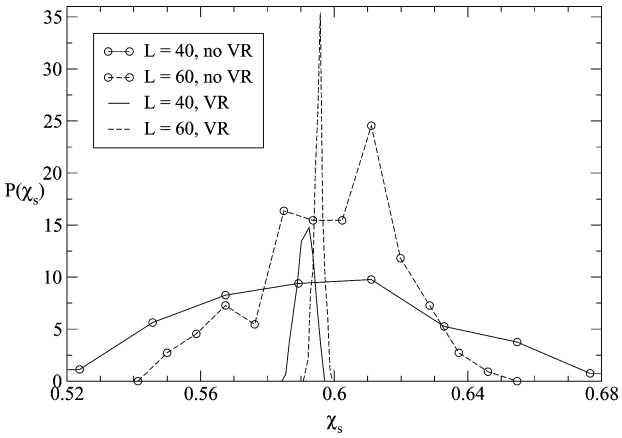

Figure 1. Distributions $P(\chi_s)$ of the incompatibility χ_s, where different realizations start to demix. The figure includes data from 128 independent realizations for each set of parameters. The value χ_s has been determined by matching the probability distribution of the order parameter m onto the universal critical 3D Ising distribution (cf. also Figure 6). The system parameters are $M = 1$, $Q = 10$, $\lambda = 0.8$, and $L = 40$ or 60 with or without variance reduction (VR). The height of the distributions with VR has been divided by a factor 10 for clarity.

In the special case where $f = 1/2$, we can merge, for even k, $C(m, k, A)$ with $C(m, k, B)$ into a class $C(m, k)$ and eq 17 becomes

$$n_C = \binom{N_A - 1}{S_A - 1}\binom{N_B - 1}{S_B - 1} + \binom{N_A - 1}{S_B - 1}\binom{N_B - 1}{S_A - 1} \quad \text{for even } k \quad (18)$$

Moreover, in ECE, we can also merge $C(m, k)$ with $C(-m, k)$ (for all k and $m \neq 0$) and, of course, the corresponding values of n_C are doubled.

We have checked the efficiency of this procedure for a choice of the parameters (namely, $Q = 10$, $M = 1$, $\lambda = 0.8$, and $L = 40$ or 60). In each case, we produced 128 samples with and without using our procedure and measured the position of the demixing transition (as described later). The distributions of the results are shown in Figure 1. As can been seen, this method dramatically reduces the fluctuations. In this case the fluctuations are reduced by a factor 20 and the final results are precise enough for our study. We thus do not need to average over the disorder, which corresponds, for the given precision, to a gain of computer time of a factor 400!

IV. Results

A. Overview of the Phase Diagram. The mean field calculations[3,5] predict a disordered phase at low values of incompatibility. For $\lambda > \lambda_L = -2 + \sqrt{3}$ one encounters a transition to a macrophase-separated state at χ_s, and then at even larger values of the incompatibility, χ_m, the A-rich and B-rich phases remix to form a spatially structured phase. The region of stability of the macrophase-separated state, $\chi_m - \chi_s$, decreases with the number of blocks as $1/Q$. For $\lambda < \lambda_L$, there is a transition between a disordered state and a lamellar phase; no two phase coexistence is predicted.

Fluctuation effects are expected to modify the mean field scenario: In particular, the isotropic Lifshitz point at $\lambda = \lambda_L$ does not survive fluctuations.[23] Fluctuations will change the order of the transition toward the microphase-separated state from second to first[24−27] and a microemulsion-like morphology is expected in the vicinity of the Lifshitz point. In the following, we investigate the phase behavior for $\lambda \geq 0$, i.e., far away from the Lifshitz point.

We use ECE (together with the disorder variance reduction) to investigate the phase diagram. As already mentioned, this ensemble is well adapted to study macrophase separation.

We investigated different values of the parameters Q, M, λ, L, and χ (always restricting ourselves to $f = 1/2$). We measured $m = (N_B - N_A)/NN_p$, the global composition of the mixture ($-1 \leq m \leq 1$). For low values of χ (i.e., large temperatures), there is always a homogeneous phase. If λ is small enough, the system stays homogeneous for all values of χ and we do not see any transition. Local correlation in the composition is gradually built up, but for sufficiently large Q, the system remains disordered in our simulation. Typical snapshots of the system at incompatibility $\chi = 0.264$, 0.473, and 0.806 are presented in Figure 2 for $Q = 5$ and $M = 4$. The types of different blocks are uncorrelated $\lambda = 0$ and the system size is $L = 120 \approx 9R_e$ (R_e being the end-to-end distance of the molecules). Mean field theories predict lamellar phases in this parameter region, while we observe a microemulsion-like structure. It is unclear whether we observe this disordered structure due to thermal fluctuations or whether the morphology is frozen-in on the time scale of our simulation and the system might eventually form an ordered lamellar structure. In any case, a complete ordering of the system would require extremely long relaxation times. We note, however, that on the time scale of our simulations, we do not even observe the onset of such an ordering but that for smaller number of blocks, $Q = 2$ and 3, and smaller system size we are able to observe the formation of a lamellar phase (cf. inset in Figure 12). As we shall see, this gradual formation of a microemulsion-like

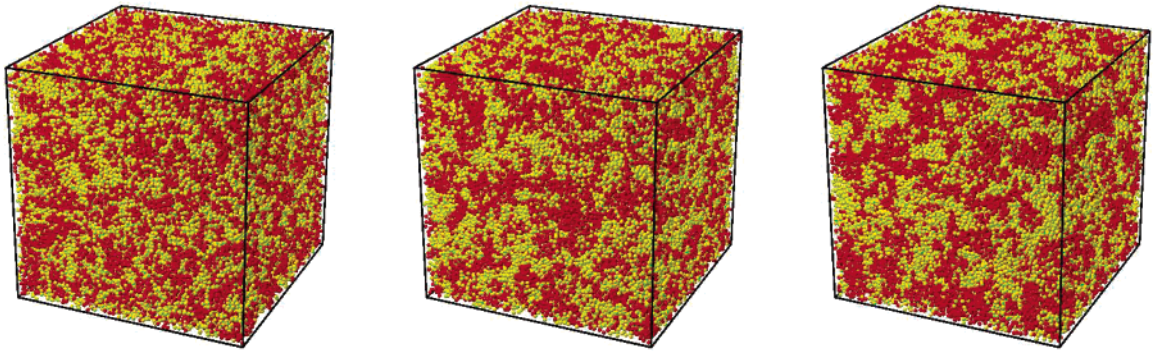

Figure 2. Typical snapshots of a random copolymer mixture for $Q = 5$, $M = 4$, and $\lambda = 0$. The incompatibility increases from left to right and takes the values $\chi = 0.267$, 0.475, and 0.806, respectively. A disordered microemulsion-like structure gradually forms upon cooling.

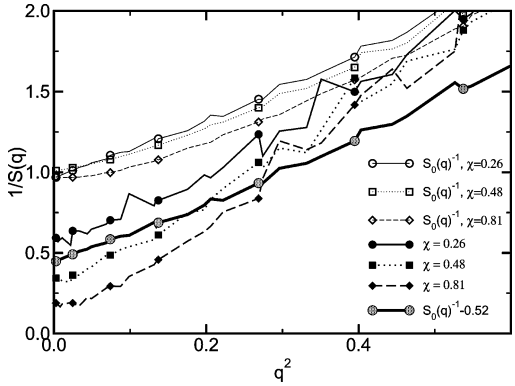

Figure 3. Inverse of the collective structure factor for the same parameters as in Figure 2. For small incompatibility we also show the inverse of the single-chain structure factor shifted by 2χ as suggested by the random phase approximation.

structure is the typical phase behavior of random copolymers over most part of the parameter region.

In the weak segregation limit one can describe the local concentration fluctuations by the random phase approximation

$$\frac{1}{S(q)} = \frac{1}{S_0(q)} - 2\chi \tag{19}$$

where $S(q)$ denotes the collective structure factor and $S_0(q)$ the single chain structure factor, where A-monomers yield a positive contribution and B-monomers a negative one. For uncorrelated blocks ($\lambda = 0$) the single-chain structure factor, S_0, is proportional to the structure factor of a single block. The behavior of the structure factor is presented in Figure 3. At small incompatibility, $\chi = 0.26$, the data are compatible with the random phase approximation. This provides evidence for a useful identification of the Flory−Huggins parameter χ in our simulation model. Upon increasing the incompatibility, the scattering at small wavevectors increases. However, the shape of the inverse structure factor changes with incompatibility and the data for larger χ cannot be obtained by a simple vertical shift of the data. Even though the system remains macroscopically homogeneous and disordered, there are strong local composition fluctuations that are not faithfully described by the random phase approximation. We recall that—in contrast to a binary homopolymer blend—the typical values of the incompatibility χ are of order unity (instead of $1/N$). These strong interactions on the monomer scale can alter the structure of the monomeric fluid. Of course, these effects cannot be captured by mean field calculations using the Gaussian chain model, where there is no explicit fluid structure and the chain conformations in the disordered phase are independent from incompatibility.

On the other hand, if λ is large, the systems separates into an A-rich phase and a B-rich phase as χ is increased. The composition difference between the two phases is only of the order $1/\sqrt{Q}$.[5] Sequences with an excess of A partition into the A-rich phase, while those which contain more B-monomers are enriched in the B-rich phase; the distribution of $N_S + N_{\bar{S}}$ is identical in both phases and agrees with the distribution in the disordered state, of course. The chain dimensions in the disordered and the macrophase-separated state are largely independent from the incompatibility. Finally, for even larger values of χ, the systems remix. This

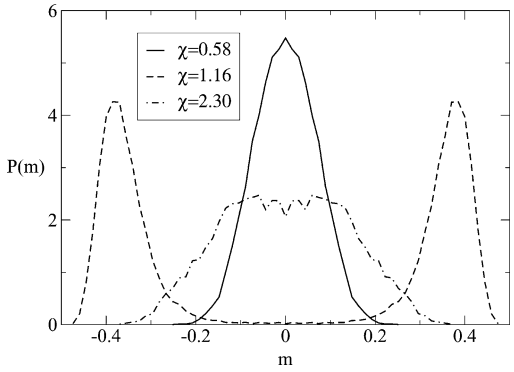

Figure 4. Distribution of m for different values of the incompatibility χ. The data here correspond to $M = 1$, $Q = 10$, $\lambda = 0.75$, and $L = 60$.

sequence of phases is illustrated by the distribution of m, whose typical shapes are shown in Figure 4. Upon increasing χ, the distribution changes from unimodal (disordered) to bimodal (A-rich and B-rich macrophases) to unimodal (remixing into a spatially structured phase).

To precisely locate the phase transitions, we use the Binder cumulant

$$g = \frac{1}{2}\left(3 - \frac{\langle m^4 \rangle}{\langle m^2 \rangle^2}\right) \tag{20}$$

which vanishes for a Gaussian distribution and is unity for a peaked bimodal distribution $P(m) = (\delta(m - m_0) + \delta(m + m_0))/2$. Thus, in the thermodynamic limit, it is 0 for a homogeneous phase and 1 for a two-phase region.

The demixing transition at low incompatibility is, according to mean field theory, a second-order phase transition. The standard method to accurately locate such a transition is to determine the crossing point of the curves $g_L(\chi)$ for different values of L, since for large L g depends only on $(\chi - \chi_s)/L^{\nu}$ and is thus constant at χ_s. Doing simulations for many L would unfortunately take much too long, so we choose another possibility. Knowing that this transition is of the Ising universality class gives us the limiting universal value of $g_L(\chi_s)$, namely, $g_\infty \simeq 0.706$. We thus simulate only one size L and determine χ_s such that $g_L(\chi_s) = g_\infty$. In practice, we use $L = 40$, 60, and 80 for $N = 5$, 10, and 20, respectively. The procedure is exemplified for $Q = 5$ and $M = 4$ in Figure 5. Moreover, we checked that at χ_s the distribution of m effectively is the Ising universal critical distribution (see Figure 6), which confirms (if needed) that this transition belongs to the Ising universality class and that our procedure is correct.

The remixing transition is a more delicate issue: According to mean field theory.[5] it should be a first-order transition at a unique value of the incompatibility χ, but there are several alternative scenarios which will be discussed in section IV.C. Not knowing the exact nature of the remixing, we arbitrarily *define* an *approximate* estimate of the location χ_m of the transition using the same criterion as before, namely, $g_L(\chi_m) = g_\infty$ which corresponds to an intermediate point between a two-peak and one-peak distribution. The results for χ_s and χ_m are presented in Figure 7. Let us analyze them in turn:

B. Demixing Transition. The scaling of χ_s as a function of Q, M, and λ can be understood using mean field results and the Ginzburg criterion. According to mean field theory,[5] we have

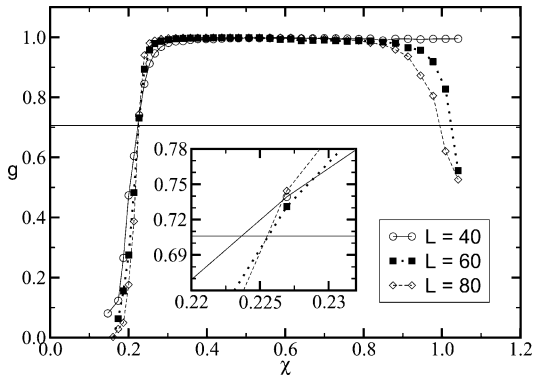

Figure 5. Temperature dependence of the Binder cumulant for $Q = 5$, $M = 4$, $\lambda = 0.7$, and system sizes $L = 40$, 60, and 80 as indicated in the key. The horizontal line marks the value of the Binder cumulant at a second-order transition of Ising type in 3 dimensions. The inset enlarges the region of the demixing transition.

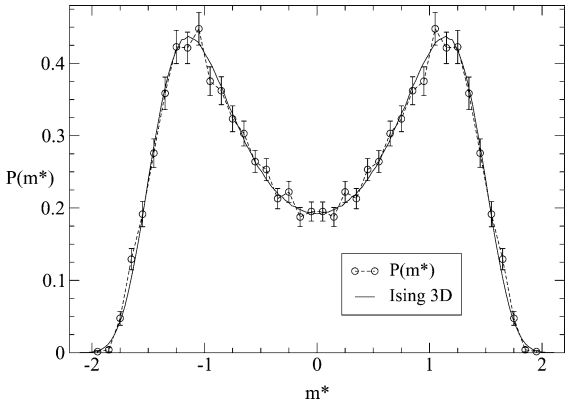

Figure 6. Distribution of $m^* = m/\sqrt{\langle (m-\langle m\rangle)^2\rangle}$ at $\chi = \chi_s$ for $M = 1$, $Q = 10$, $\lambda = 0.8$, and $L = 60$. The solid curve is the universal Ising critical distribution in a cubic cell.

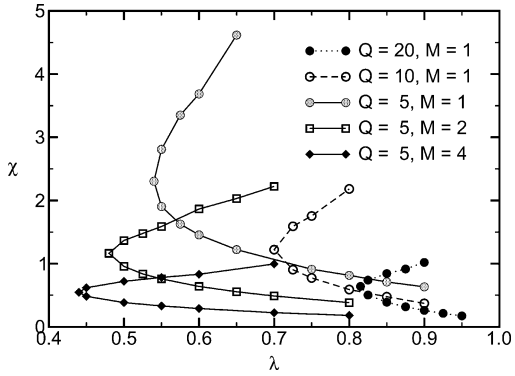

Figure 7. Summary of the simulation results for the location of the demixing transition (at low incompatibility) and the remixing transition (at larger χ). The location of both transitions has been estimated by the value of the Binder cumulant of m (cf. Figure 5). This yields an accurate estimate for the demixing transition but only a rough estimate for the remixing.

$$\chi_s = \frac{2}{\Lambda M} \tag{21}$$

where $\Lambda = (1 + \lambda)/(1 - \lambda)$ is such that

$$\langle m^2 \rangle = \Lambda M^2 Q \tag{22}$$

in the limit of large Q (m is the excess of A in one polymer). In our case, we have relatively short polymers and we need the small Q corrections to Λ, namely

$$\Lambda = \frac{1+\lambda}{1-\lambda} + \frac{2\lambda(\lambda^Q - 1)}{(1-\lambda)^2 Q} \tag{23}$$

such that eq 22 is exact for all Q (eq 21 is thus compatible with eq 7 of ref 4 for $M = 1$ and $f = 1/2$ or eq 3.10 of ref 5.).

As already argued in ref 7, fluctuations have a pronounced influence on the demixing transition. Their importance can be gauged from the Ginzburg criterium:[8] The mean field theory is correct if the fluctuations of the composition inside a volume of the correlation length, ξ, are small compared to the difference in composition of the two coexisting phases. Both the composition and its fluctuations as well as the spatial correlation length can be calculated from mean field theory. It is instructive to compare the results to a binary blend of homopolymers. Let $t = (\chi - \chi_s)/\chi_s$ denote the distance to the unmixing transition, then the composition difference between the two coexisting phases scales as $\Delta\phi \approx t^{1/2}/\sqrt{Q}$ in the case of random copolymers. The critical amplitude is reduced by the factor $1/\sqrt{Q}$ compared to homopolymer blends to account for the typical difference in composition between different species. The correlation length of composition fluctuations scales as $\xi \approx R_M t^{-1/2}$, where R_M denotes the size of a block. In case of a homopolymer blend, the length scale is proportional to the chain extension $R_N \approx QR_M$. Likewise, the strength of composition fluctuations is given by the susceptibility $\tilde{\chi} \approx M/(\rho t)$, while in the homopolymer blend the amplitude is proportional to $N = QM$. The Ginzburg criterion $(\Delta\phi)^2 \gg \tilde{\chi}\xi^{-3}$ then yields[7]

$$t \gg \mathrm{Gi} = \frac{16}{\Gamma^3} Q^2 \left(\frac{M}{\rho R_M^{\,3}}\right)^2 \tag{24}$$

where we have included the dependence on λ using

$$\Gamma = \frac{\lambda^2 + 4\lambda + 1}{3(1-\lambda^2)} \tag{25}$$

The radius of gyration of a block is given by $R_M^{\,2} = l_b^{\,2} M$ with $l_b^{\,2} \simeq 1.5$. Here again, we need to correct eq 24 to take into account the actual finite interaction range of the bond fluctuation model. Thus, the factor $\Gamma R_M^{\,2}$ in eq 24, which is the coefficient of the square gradient term, must be replaced by $\Gamma R_M^{\,2} + l_0^{\,2}/2$, where $l_0^{\,2} = 14/9$ (in units of the lattice spacing). The Ginzburg parameter thus becomes

$$\mathrm{Gi} = \frac{16N^2}{\rho^2(\Gamma R_M^{\,2} + l_0^{\,2}/2)^3} \tag{26}$$

and we expect a shift of the transition of the order $\sqrt{\mathrm{Gi}}$[20,28,29]

$$\chi_s \simeq \frac{2}{\Lambda M}(1 + a\sqrt{\mathrm{Gi}} + \cdots) \tag{27}$$

where a is some constant.

Figure 8 shows the corresponding scaling behavior. The data are in good agreement with eq 27: The lower part of the curves (i.e., χ_s) collapse nicely together onto a straight line. The intercept of this line at $\mathrm{Gi} = 0$ is slightly larger than the expected value 2. This discrepancy is due to different reasons: (i) The polymers used

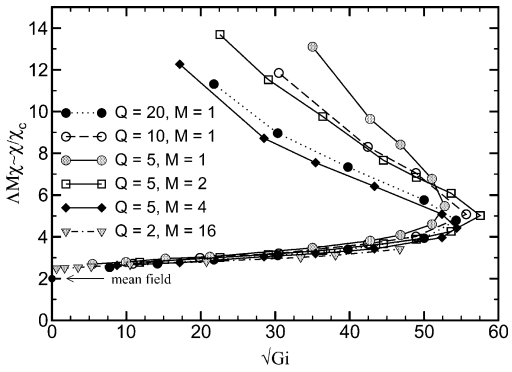

Figure 8. Phase diagram with rescaled variables $\sqrt{\mathrm{Gi}}$ and $\Lambda M\chi$ as suggested by the Ginzburg criterion, eq 27. The data for the demixing transition for all parameter combinations shown in Figure 7 collapse onto a unique curve in this representation.

are quite short $N \leq 20$, (ii) M is very small (1, 2, or 4) and our values for R_M are not accurate, (iii) eq 25 for Γ is valid only for $\lambda^Q \ll 1$ and would also require some corrections (we unfortunately do not know how to compute them).

In Figure 8, we also show the results for the Scott line from ref 19 (Table 2), which corresponds to $Q = 2$ and $M = 16$. It is surprising to see how good the scaling is, even for the smallest value of Q. Note that for $Q = 2$ the relative concentration ρ_c of copolymers is related to λ through $\lambda = 1-2\rho_c$. According to eq 23, $\Lambda = 1 + \lambda$ for $Q = 2$ and the mean field equation for the Scott line $(1 - \rho_c)M\chi_s = 2$ exactly yields eq 21.

To summarize, the demixing transition at low values of incompatibility is a second-order transition that belongs to the 3D Ising universality class. It is strongly affected by fluctuations, and the strength of the fluctuations can be described by the Ginzburg parameter. Our simulation corroborates the Ginzburg criterion for a wide range of parameters. Concerning the rest of the data, namely, χ_m and the turning points, the scaling has a priori no reason to apply.

C. Remixing Transition. In the previous section we used the same criterion (i.e., matching the shape of $P(m)$ onto the universal 3D Ising curve) as for the second-order unmixing transition at low χ to investigate remixing at large incompatibilities. It would be illusory to accurately locate the remixing transition without understanding its nature. One may envisage different possible scenarios: (i) A second-order transition of Ising type, (ii) a first-order transition, (iii) an unbinding transition, or (iv) a three-phase region as predicted by Nesarikar et al.[6] and Subbotin and Semenov.[30] In principle, one could imagine even more complicated possibilities such as, for instance, an infinite series of transitions with 3, 4, 5,... coexisting phases.[6] Remember that theoretically an infinite number of phases can coexist in the limit $Q \rightarrow \infty$. While we cannot exclude this possibility from the outset, it is certainly not feasible to observe such complicated possibilities using the simulation technique of the present study. Therefore, we restrict our attention to scenarios i−iv.

(i) If the transition was of second order, the segregation between the A-rich and B-rich macrophases would continuously decrease as we approached the remixing transition. As the transition would be characterized by a single scalar order parameter, m, we expected it to be of Ising type. Using finite size scaling techniques we could locate the transition temperature. In Figure 5 we presented the Binder cumulants of $P(m)$ as a function of the incompatibility χ for $\lambda = 0.7$ and different system sizes. While there is a rather well-defined intersection at low values of χ (demixing) and the value of the cumulants at the common intersection nicely agrees with the universal value of the 3D Ising universality class, no such intersection point of the cumulants for different system sizes can be detected at the remixing transition. From this figure we conclude that the transition is not a second-order transition of Ising type. This also clearly illustrates that our estimate used in section IV.A is only a very rough approximation.

(ii) Mean field calculations of Fredrickson and coworkers[5] suggest that at a single value of incompatibility there is a three-phase coexistence between the two macroscopically segregated phases and the lamellar phase. At lower incompatibility an A-rich and a B-rich phase coexist, while at larger χ a spatially structured phase is stable. The sequence distribution of that spatially structured phase is a λ distribution (cf. section II.A). If the three phases coexist, however, we expect that the sequence distributions in the phases will differ: The sequences with larger values of k will partition into the lamellar phase, while those sequences with smaller k or larger excess of A- or B-monomers will partition into the corresponding macroscopically segregated phases. This fractionation is in accord with our simulation results (cf. below), and its has been considered by refs 6 and 30. Therefore, we can also rule out the possibility of a three-phase coexistence at a single value of incompatibility.

(iii) In the unbinding scenario, the length scale D of the spatially structured phase continuously diverges as one approaches the transition from high values of incompatibility χ. The A-rich regions of the spatially structured phase (lamellar or microemulsion) can be conceived as the macroscopically A-rich phase in the limit $D \rightarrow \infty$.

Such a scenario has been predicted for mixtures of two homopolymers and a symmetric diblock at intermediate values of segregation. This corresponds to the special case $Q = 2$ in our model, the concentration of copolymers ρ_c being related to the parameter λ via $\lambda = 1-2\rho_c$. In fact, our phase diagrams in Figure 7 are topologically similar to the mean field prediction of Janert and Schick:[31,32] For $\rho_c < 2/3$, the mixture of two homopolymers and a symmetric diblock copolymer macrophase separates into an A-rich and a B-rich phase upon increasing the incompatibility χ. This Scott line corresponds to the demixing transition investigated in the previous paragraph. Upon increasing χ further at sufficiently large copolymer concentration, one encounters an unbinding transition. Upon increasing χ at small values of ρ_c, one encounters a three-phase coexistence between two homopolymer-rich phases and a lamellar phase of finite lamellar spacing D. For $\rho_c > 2/3$ there is a direct transition from disordered phase to lamellar phase. At $\rho_c = 2/3$ there is a tricritical Lifshitz point where fluctuations become very important and destroy the lamellar ordering. In simulations and experiments, one observes a microemulsion-like structure in the vicinity of the Lifshitz point. In the ternary mixture, however, mean field theory will become exact in the limit of large chain length and the Ginzburg number[34,35] at the tricritical Lifshitz point scales as $\mathrm{Gi} \approx (\rho R_N^3/N)^{-4/3}$.

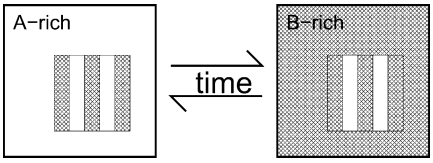

Figure 9. Illustration of three-phase coexistence in the ECE.

Due to the diverging length scale D, this unbinding transition is difficult to observe in simulation. On the one hand, one has to equilibrate long-range fluctuations which have extremely long relaxation times. On the other hand, we expect very pronounced finite size effects due to the diverging length scale D.

(iv) Alternatively, the remixing transition could proceed via a three-phase coexistence, where the A-rich and B-rich macrophases would coexist with a spatially structured phase of finite length scale D over an extended range of incompatibilities. Upon increasing the incompatibility χ, the third spatially structured phase would form initially in an infinitesimal fraction of the total volume. Upon increasing χ further, the volume fraction of the spatially structured phase would increase and the volume fractions of the two macrophase-separated phases would decrease. The composition of the phases also gradually changes in this temperature regime. At large χ, the volume fraction of the macrophases might vanish and only the spatially structured phase would remain. This three-phase scenario corresponds to the behavior of a homopolymer−copolymer mixture, $Q = 2$, at large χ and low concentration of copolymers. A three-phase coexistence between an A-rich, a B-rich phase, and a spatially structured phase has also been suggested for random copolymers by Subbotin and Semenov,[30] while Nesarikar et al.[6] assumed the third phase to be homogeneous.

Observing this three-phase coexistence in computer simulation is difficult. The extended canonical ensemble (ECE) is not adapted to investigate the possibility of a three-phase coexistence. The spatially structured phase will form in the A-rich and B-rich macrophases as illustrated in Figure 9. As the segregation of the macrophases is weak (for large number of blocks, Q), we expect the interface between the macrophases and the spatially structured phase to be very broad and substantially influence the properties in a finite-sized simulation box. Increasing the incompatibility in the three-phase region, one would observe that the two peaks of the distribution $P(m)$ gradually moved close to the symmetric value and eventually formed a single peak centered around $m = 0$ as one would leave the three-phase region and the volume fraction of the macrophase-separated phases would vanish. Qualitatively, the behavior of $P(m)$ looked similar to a second-order transition, but there would be no critical behavior, and therefore the Binder cumulants would not cross. This is in accord with our simulation results in Figure 5.

On the one hand, one could perform Gibbs ensemble calculations with three simulation boxes. Such simulations have been performed by Poncela, Rubio, and Freire for a homopolymer−copolymer mixture, $Q = 2$.[36] In principle, the scheme is well suited for each phase resides in an individual simulation box and surface effects can be avoided. In addition to moves that transfer polymers from one box to another, the simulation algorithm has to include moves that transfer volume between the boxes[37]—note that the volume fractions of the three phases are not given by symmetry and do vary as a function of incompatibility. While these volume changes can rather efficiently be implemented in off-lattice models, such moves in a lattice model are a tour de force. (Of course, the use of an off-lattice model would make the implementation of volume exchange moves not much more computationally expensive than the other Monte Carlo moves. However, overall the simulation would require an order of magnitude more CPU time because the calculation of the energy difference cannot be implemented as efficiently as in our lattice model.)

On the other hand, one could perform semi-grand-canonical simulations. At three-phase coexistence we would observe the system in each of the three phases in the course of the simulation. The time the system spends in each phase is proportional to the volume fraction of this phase. As mentioned in section III.A, this is in principle an elegant method but requires knowledge of the chemical potentials of the different species and is therefore limited to small values of Q. We have chosen this method.

1. $Q = 2$: Homopolymer−Copolymer Mixture. To exemplify our simulation technique and illustrate possible finite size effects, we first discuss the case $Q = 2$, i.e., a mixture of two homopolymers and a symmetric AB diblock copolymer. Restricting us to the isopleth ($\mu_S = \mu_{\bar{S}}$), a single chemical potential $\delta\mu$ remains that controls the relative concentration ρ_c of the diblock copolymer in the semi-grandcanonical ensemble.

In Figure 10a we present the joint probability distribution of m and the concentration of copolymers, ρ_c. At low incompatibility χ, the probability distribution exhibits two peaks at $\rho_c = (1 - \lambda)/2$ and positive and negative values of m, respectively. This is the macrophase coexistence discussed in section III.B. Upon increasing the incompatibility further, we can distinguish clearly three peaks associated with two almost pure homopolymer-rich phases and a third phase with equal number of A and B blocks and a large content of copolymers. This distribution corresponds to an apparent three-phase coexistence; it is the generic type of distribution that we observe in our simulations at intermediate and high values of the incompatibility.

Figure 10b shows the apparent phase diagram as a function of λ and incompatibility χ. The line at low χ corresponds to the Scott line, which marks the onset of macrophase separation. At higher incompatibility, the three-phase coexistence comprises two homopolymer-rich phases at λ very close to unity and a spatially structured phase at high copolymer content or smaller values of λ, respectively. The figure shows two sets of data extracted from systems of different sizes. While our estimate for the location of the Scott line does not depend on the system size (note that we have accounted for finite size effects at the second-order transition in our analysis), our estimate for the spatially structured copolymer-rich phase exhibits a strong dependence on the system size. The larger the system size, the higher the homopolymer concentration in the copolymer-rich phase. These surprisingly large finite size effects make it difficult to distinguish between a true three-phase region and an unbinding transition. If the concentration of the copolymer-rich phase tends toward the concentration of the two homopolymer-rich phases (which do hardly exhibit any dependence on the system size), the transition will be of unbinding type. If the concentration ρ_c of the copolymer-rich phase adopts a value larger than

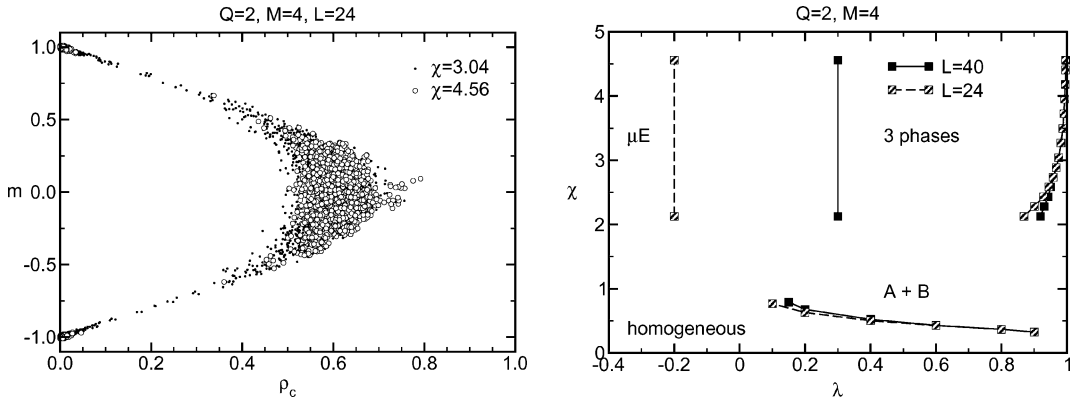

Figure 10. (a) Joint probability distribution of the order parameter m and the density of copolymers ρ_c for $Q = 2$, $M = 4$, $L = 24$, and two values of χ as indicated in the key. (b) Apparent phase diagram for the homopolymer−diblock mixture for two different system sizes. While our estimate for the demixing transition (Scott-Line) has not exhibited strong finite size effects, our estimate for the copolymer concentration of the symmetric, copolymer-rich phase depends on L.

the homopolymer-rich phases in the limit of infinite system size, there will be a true three-phase coexistence. For any finite system size, however, we observe an apparent three-phase region and only via a finite size analysis we can distinguish between an unbinding transition and a true three-phase coexistence.

To extrapolate our simulation data to infinite system size, we propose a phenomenological finite size scaling. If the transition is of unbinding type, we will observe an apparent three-phase coexistence in the simulation when the characteristic length scale of the spatially structured phase D is on the order of the system size L. Hence, the interfacial area is on the order of L^2. If the system size is large enough, we can conceive the spatially structured phase as an assembly of interfaces that separate domains in which the concentration ρ_c corresponds to the concentrations in the spatially homogeneous, homopolymer-rich phases, $\rho_c^{\text{coex}-}$. For the parameters chosen in the simulation, $\rho_c^{\text{coex}-}$ is nearly zero. The interfaces in the spatially structured phase carry an excess of copolymers, σ_c. We expect the concentration of the copolymer-rich phase at the apparent three-phase coexistence to depend like

$$\rho_c = \rho_c^{\text{coex}-} + \frac{\sigma_c}{D} = \rho_c^{\text{coex}-} + \frac{const}{L} \qquad (28)$$

on the system size L for an unbinding transition. In the case of a true three-phase coexistence, however, the copolymer concentration eventually becomes independent from the system size L because D remains finite.

In Figure 11 we plot the copolymer concentration of the copolymer-rich phase as a function of $1/L$ for $Q = 2$, $M = 4$, and $\chi = 4.56$. Indeed, the simulation data are nicely compatible with a finite size scaling of eq 28. This does not prove the existence of an unbinding transition: The data for $\rho_c(L)$ could still approach an asymptotic value that is larger than $\rho_c^{\text{coex}-}$. Such a behavior would correspond to a three-phase coexistence that comprises a spatially structured phase with a characteristic length scale D that exceeds (or is comparable to) the largest system size studied. Note, however, that the system size is about $L \approx 4.8R_e$, a value that has to be compared to the location of a possible minimum in the binding potential of two lamellae. Naughton and Matsen[33] observed such a minimum at $D \leq 3R_e$ for $\chi N = 11$. Even though our simulations are at a slightly higher incompatibility (where all mean field calculations expect a three-phase coexistence), this length scale

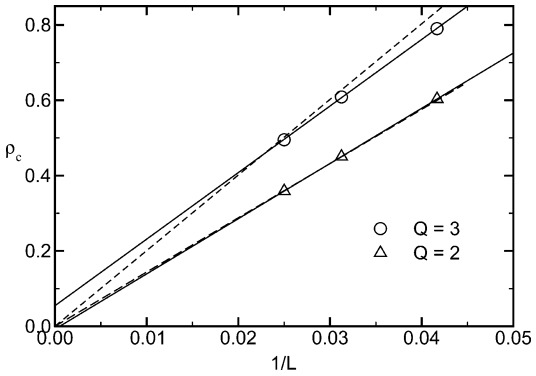

Figure 11. Phenomenological finite size scaling of the concentration of the copolymer-rich phase for $Q = 2$, $M = 4$, and $\chi = 4.56$ and $Q = 3$, $M = 4$, and $\chi = 4.25$. The data show linear regressions to the data (solid lines) and tentative behavior compatible with an unbinding transition (dashed lines). For $Q = 2$ the data provide evidence for an unbinding transition, while the data for $Q = 3$ lend support to a three-phase coexistence.

yields an estimate for a system size beyond which we expect the characteristic behavior of an infinite system. Therefore, the data present strong evidence for an unbinding transition in the homopolymer−diblock mixture.

2. $Q = 3$: Three-Phase Coexistence and Fractionization. The joint probability distribution of m and ρ_c is shown in Figure 12 for the six-component mixture with $Q = 3$. In this case one has to tune two independent chemical potentials to locate the apparent three-phase coexistence region. It looks qualitatively similar to the case $Q = 2$. The figure also includes typical snapshots from the simulation. Notably, the copolymer-rich phase has a lamellar-like structure with a characteristic length scale on the order of the system size. Figure 11 also includes the corresponding data for $Q = 3$. The concentration of the copolymer-rich phase is compatible with a $1/L$ dependence and yields an estimate for the asymptotic value of the copolymer concentration in the limit $L \to \infty$ that is larger than the concentration of the homopolymer-rich phases. Therefore, the data suggest that one would observe a three-phase coexistence in the thermodynamic limit. Of course, the same caveats apply to this conclusion as for a mixture with $Q = 2$. Additionally, the data for small system sizes might not obey the simple $1/L$ relation because ρ_c cannot exceed unity. This effect would lead to an overestimation of the true asymptotic value of the copolymer concentration. An

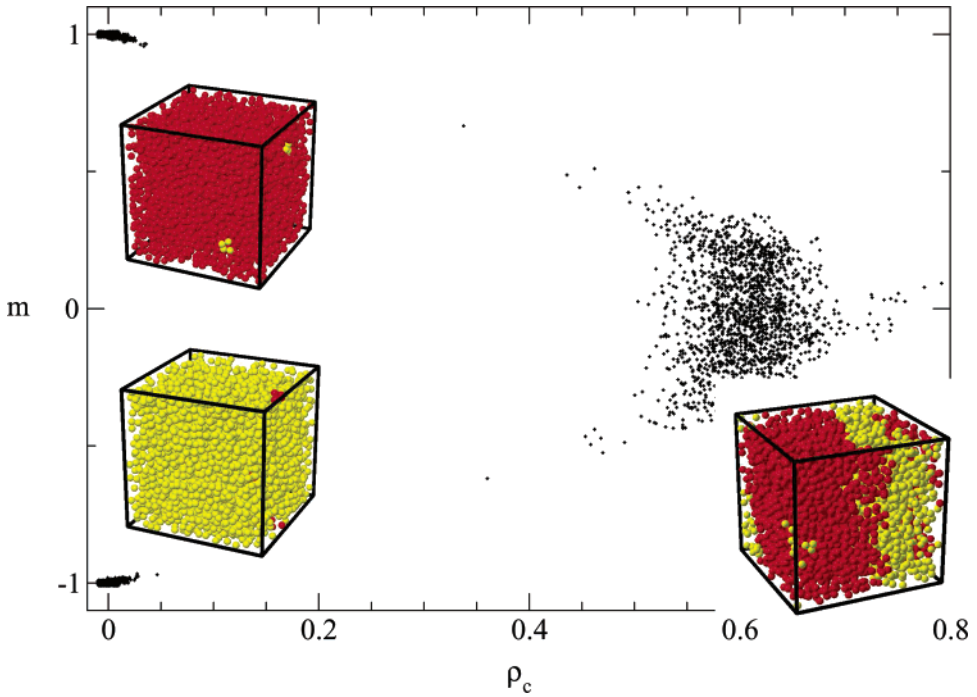

Figure 12. Joint probability distribution of the order parameter m and the copolymer density ρ_c for $Q = 3$, $M = 4$, $L = 40$, and $\chi = 4.245$. The snapshots illustrate the typical configuration of the A-rich phase, B-rich phase, and copolymer-rich (lamellar) phase.

alternative $1/L$ dependence with a lower value of the asymptotic copolymer concentration (consistent with an unbinding transition) is also shown in the figure but yields a significantly worse description of the simulation data. Additionally, we do not have a heuristic argument for extrapolating the data with $1/L$ toward the asymptotic limit for a true three-phase coexistence. Alternatively, one could expect that the finite size effects of the concentration scale like $L^{-3/2}$ as for an ordinary first-order transition. The simulation data do not cover a sufficient range of system sizes to distinguish between those two alternatives. We note, however, that an extrapolation with $L^{-3/2}$ would yield an even larger estimate of the asymptotic value of the asymptotic copolymer concentration in the copolymer-rich phase. Despite all these caveats, the simulation data are best compatible with a true three-phase coexistence in the case $Q = 3$.

Let us assume for the remainder that there was a true three-phase coexistence and discuss the consequences of such a scenario: As mentioned above, if we cool a mixture with a fixed value of λ, we do not observe a transition between the macrophase-separated regime and the spatially structured phase at a single value of the incompatibility as suggested by the mean field calculations but there is an extended region of incompatibilities where the three phases coexist. The behavior is similar to a polydisperse polymer solution where one identifies cloud and shadow curves as the onset of liquid−vapor coexistence and the incipient phase, respectively. As in polydisperse systems, the different species partition differently into the coexisting phases and the distribution in each of the phases cannot be characterized by a value of λ: Species with a larger number of AB bonds, k, will be enriched in the copolymer-rich phase, while those polymers which resemble most homopolymers will be preferentially found in the homopolymer-rich phases. For a mixture with $Q = 3$, this fractionation is shown in Figure 13. We can group the polymers into three different groups: Homopolymers AAA and BBB, diblock copolymers ABB and BAA, and triblock copolymers ABA and BAB. The concentrations of the three groups add to unity. A distribution of the type discussed in section II.A, λ-distribution, corresponds to a single point in the concentration triangle in Figure 13. All those distributions with different values of λ form the line in the concentration triangle. In panel a we present the situation where the copolymer-rich phase is incipient, i.e., in the two-dimensional distribution we can just locate the indication of a peak. The composition distribution of the incipient phase (shadow phase) cannot be described by the value of λ. The homopolymer-rich phases, in turn, occupy almost all volume and are characterized by a value of λ.

The simulation data at three-phase coexistence (which correspond to the two peaks in the figure because the peaks that correspond to the two macroscopically segregated phase collapse onto each other in this diagram) are presented in panel b. Each peak has an equal statistical weight. None of the phases lie on the λ-line. In accord with intuition, the ratio of triblocks to diblocks is higher in the copolymer-rich phase than in the homopolymer-rich phase. This fractionation of the distribution at the three-phase coexistence might be useful to tailor the sequence distribution.

V. Conclusion and Outlook

Using large-scale Monte Carlo simulations we investigated the phase behavior of a dense melt of random AB copolymers. Even though we restricted ourselves to situations which are symmetric with respect to the transformation A ⇌ B, the accurate study of the phase behavior poses a computational challenge due to the presence of weakly segregated macrophases and spatially structured phases with a large characteristic length scale. We devised several Monte Carlo techniques to specifically cope with these problems: To efficiently equilibrate the polymer conformations we used a worm-

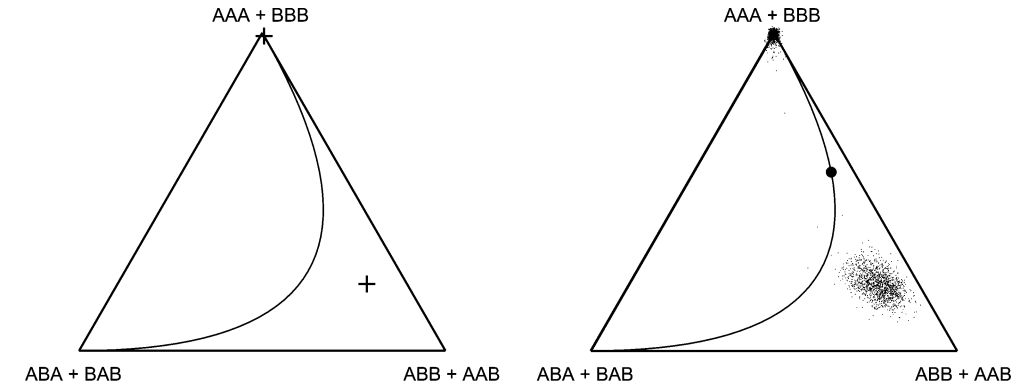

Figure 13. Composition triangle for $Q = 3$, $M = 4$, $L = 24$, and $\chi = 4.25$. Species which are related by symmetry have been grouped together. (a) The chemical potentials have been chosen such that the homopolymer-rich phases correspond to a distribution that is characterized by a λ value. For these parameters the copolymer-rich phase is just about to appear. The cross marks the distribution of the incipient copolymer-rich phase (shadow). It is far away from the line that describes all λ-distributions. (b) The chemical potentials have been chosen such that all three phases have approximately equal weight. None of the phases can be described as a λ-distribution, but the sum of all phases corresponds to $\lambda = 0.5$ (as indicated by the circle on the λ-line). The symbols mark the different compositions during the simulation run. They are scattered over a small region in order to avoid crowding.

hole move that generalizes the slithering-snake algorithm to polymers with a fixed random sequence.[14] Conceiving the random copolymer melt as a mixture with many components, we explored a scheme to select the sequences in a finite-sized simulation box. This disorder variance reduction yields the exact result in the thermodynamic limit but reduces the fluctuations between different finite-sized samples. Various statistical ensembles have been used to study phase coexistence.

In contrast to mean field calculations by Fredrickson and co-workers,[5] random copolymers that contain many blocks Q gradually form a disordered microemulsion-like structure upon increasing the incompatibility. There is no macrophase separation for large Q. Only for small Q we observe macrophase separation into weakly segregated macrophases. The location of this demixing transition is strongly affected by fluctuations. They can be described by a Ginzburg parameter $\mathrm{Gi} \approx Q^2/M$. In marked contrast to homopolymer blends, the Ginzburg parameter does not vanish for large polymers that strongly *interdigitate*.[7] Varying the number of blocks Q, their correlation λ, and the block size M, we confirm the dependence of the deviation from the mean field prediction on the Ginzburg number.

At high incompatibility χ, the two coexisting macrophases remix and form a single spatially structured phase. For all system sizes accessible to simulations, we observe an apparent three-phase region where an A-rich phase, a B-rich phase, and a symmetric, spatially structured phase coexist over an extended regime of χ values. This phase coexistence could only be studied for small values of $Q = 2$ and 3. Unexpectedly, the phase boundaries strongly depend on the system size due to the large characteristic length scale of the symmetric phase. We used a phenomenological finite size scaling to extrapolate our simulation data to infinite system size. For $Q = 2$—a homopolymer−diblock mixture—the data are compatible with an unbinding transition at an intermediate value of incompatibility. For $Q = 3$—a mixture of homopolymers, diblocks, and triblocks—the simulation results point toward a true three-phase coexistence. The sequence distribution in the three coexisting phases differs, the A-rich and B-rich phases contain more homopolymers, and the symmetric but spatially structured phase contains more triblock copolymers. As a result of this fractionation the distributions cannot be characterized by a single value of λ, i.e., the phase diagram cannot be represented in the $\lambda-\chi$ plane. The situation resembles phase separation in polydisperse systems, and techniques explored in this context (e.g., the method of moments by Sollich and co-workers[1]) might prove useful to investigate the behavior for larger values of Q.

Acknowledgment. It is a great pleasure to thank K. Binder, I. Erukhimovich, B. Vollmayr-Lee, A. Yethiraj, and A. Zippelius for stimulating discussions. J.H. thanks the Max Planck Society for a fellowship, and M.M. was supported by a Heisenberg fellowship Mu1674/1. Generous allocation of CPU time at the NIC Julich and HLR Stuttgart is acknowledged.

References and Notes

(1) Sollich, P. *J. Phys.: Condens. Matter* **2002**, *14*, R79.
(2) Pernot, H.; Baumert, M.; Court, F.; Leibler, L. *Nat. Mater.* **2002**, *1*, 54.
(3) Shakhnovich, E. I.; Gutin, A. M. *J. Phys. Fr.* **1989**, *50*, 1843.
(4) Fredrickson, G. H.; Milner, S. T. *Phys. Rev. Lett.* **1991**, *67*, 835.
(5) Fredrickson, G. H.; Milner, S. T.; Leibler, L. *Macromolecules* **1992**, *25*, 6341.
(6) Nesarikar, A.; Olvera de la Cruz, M.; Crist, B. *J. Chem. Phys.* **1993**, *98*, 7385. Wald, C.; Vollmayr-Lee, B.; Zippelius, A. Manuscript in preparation, 2003.
(7) Houdayer, J.; Müller, M. *Europhys. Lett.* **2002**, *68*, 660.
(8) Ginzburg, V. L. *Sov. Phys. Solid State* **1960**, *1*, 1824. de Gennes, P. G. *J. Phys. Lett. (Paris)* **1977**, *38*, L-441. Joanny, J. F. *J. Phys. A* **1978**, *11*, L-117. Binder, K. *Phys. Rev. A* **1984**, *29*, 341.
(9) Dobrynin, A. V.; Erukhimovich, I. Y. *JETP Lett.* **1991**, *53*, 570.
(10) Gutin, A. M.; Sfatos, C. D.; Shakhnovich, E. I. *Phys. Rev. E* **1995**, *51*, 4727.
(11) Sfatos, C. D.; Shakhnovich, E. I. *Phys. Rep.* **1997**, *288*, 77.
(12) Swift, B. W.; Olvera de la Cruz, M. *Europhys. Lett.* **1996**, *35*, 487.
(13) Hukushima, K.; Nemoto, K. *J. Phys. Soc. Jpn.* **1996**, *65*, 1604.
(14) Houdayer, J. *J. Chem. Phys.* **2002**, *116*, 1783.
(15) The thermodynamic limit is taken to be $\mathcal{V} \to \infty$ at fixed number of blocks Q per chain. We note that for large $Q \approx \mathcal{O}(100)$ there are so many different species $\mathcal{O}(2^Q)$ that even experimental samples might not be large enough to contain each species in a large number. Of course, this hold a fortiori for finite size simulation cells (cf. section III.C).
(16) Carmesin, I.; Kremer, K. *Macromolecules* **1988**, *21*, 2819. Deutsch, H.-P.; Binder, K. *J. Chem. Phys.* **1991**, *94*, 2294.

(17) Müller, M. *Macromol. Theory Simul.* **1999**, *8*, 343.
(18) Werner, A.; Schmid, F.; Müller, M.; Binder, K. *Phys. Rev. E* **1999**, *59*, 728.
(19) Müller, M.; Schick, M. *J. Chem. Phys.* **1996**, *105*, 8885.
(20) Müller, M.; Binder, K. *Macromolecules* **1995**, *28*, 1825. Müller, M. *Macromolecules* **1995**, *28*, 6556.
(21) Wilding, N. B.; Sollich, P. *J. Chem. Phys.* **2002**, *116*, 7116.
(22) Escobedo, F. A. *J. Chem. Phys.* **2001**, *115*, 5642 and 5653.
(23) Dobrynin, A. V.; Leibler, L. *Europhys. Lett.* **1996**, *36*, 283. Dobrynin, A. V.; Leibler, L. *Macromolecules* **1997**, *30*, 4756.
(24) Sfatos, C. D.; Gutin, A. M.; Shakhnovich, E. I. *J. Phys. A* **1994**, *27*, L-411.
(25) Gutin, A. M.; Sfatos, C. D.; Shakhnovich, E. I. *J. Phys. A* **1994**, *27*, 7957.
(26) Dobrynin, A. V.; Erukhimovich, I. Y. *J. Phys. I (Fr.)* **1995**, *5*, 365.
(27) Dobrynin, A. V. *J. Chem. Phys.* **1997**, *107*, 9234.
(28) Fisher, M. E. *Rev. Mod. Phys.* **1974**, *46*, 587.
(29) Mon, K. K.; Binder, K. *Phys. Rev. E* **1993**, *48*, 2498.
(30) Subbotin, A. V.; Semenov, A. N. *Eur. Phys. J* **2002**, *7*, 49.
(31) Janert, P. K.; Schick, M. *Macromolecules* **1997**, *30*, 3916.
(32) Recent self-consistent field calculations by Naughton and Matsen[33] find a small minimum in the binding potential at finite D over the entire range of incompatibility, leading to a three-phase coexistence between a lamellar phase and two homopolymer-rich phases. The minimum is, however, so weak that thermal fluctuations can easily overcome this minimum, and therefore, it is immaterial for our Monte Carlo results.
(33) Naughton, J. R.; Matsen, M. W. *Macromolecules* **2002**, *35*, 8926.
(34) Hołyst, R.; Schick, M. *J. Chem. Phys.* **1992**, *96*, 7728.
(35) Müller, M.; Gompper, G. *Phys. Rev. E* **2002**, *66*, 041805.
(36) Poncela, A.; Rubio, A. M.; Freire, J. J. *J. Chem. Phys.* **2002**, *118*, 425.
(37) Mackie, A. D.; Panagiotopoulos, A. Z.; Kumar, S. K. *J. Chem. Phys.* **1995**, *102*, 1014.
(38) Fredrickson, G. H.; Sides, S. W. *Macromolecules* **2003**, *36*, 5415.

MA035814P